

Rapid Communications

The Rapid Communications section is intended for the accelerated publication of important new results. Manuscripts submitted to this section are given priority in handling in the editorial office and in production. A Rapid Communication may be no longer than 3½ printed pages and must be accompanied by an abstract. Page proofs are sent to authors, but, because of the rapid publication schedule, publication is not delayed for receipt of corrections unless requested by the author.

Observation of Cu NMR and spin canting in antiferromagnetic $\text{CuCl}_2 \cdot 2\text{H}_2\text{O}$

Takeji Kubo and Hisashi Yamahaku

Department of Physics, Nara University of Education, Nara 630, Japan

(Received 22 April 1985)

The four-sublattice structure with small hidden spin canting in antiferromagnetic $\text{CuCl}_2 \cdot 2\text{H}_2\text{O}$ is confirmed to have a canting angle $\Delta\theta = 6^\circ \pm 1^\circ$ away from the a axis towards the c axis from the numerical analysis of the zero-field spectra of the Cu NMR in $\text{CuCl}_2 \cdot 2\text{H}_2\text{O}$ crystals. The D_b component (-0.28 K) of the vector \mathbf{D} in $\mathbf{D} \cdot (\mathbf{S}_1 \times \mathbf{S}_2)$ is also obtained. The dependence of the Cu NMR frequencies on the external field along the a axis can be reasonably interpreted by taking into account the zero-field Cu NMR results, together with an abrupt change at the spin-flop transition (6.6 kOe) at 1.5 K.

Since antiferromagnetic spin ordering in $\text{CuCl}_2 \cdot 2\text{H}_2\text{O}$ was confirmed by Poulis and Hardeman¹ using proton NMR, the compound has been extensively investigated leading to findings of new fundamental evidence concerning the antiferromagnetism, i.e., Néel temperature,² spin-flop transition,^{1,2} antiferromagnetic resonance absorption,³ etc. For $\text{CuCl}_2 \cdot 2\text{H}_2\text{O}$ the magnetic structure below $T_N = 4.33$ K has the Cu^{2+} spins coupled antiferromagnetically in the c direction but ferromagnetically in the a - b plane with the easy direction (a axis). Neutron diffraction experiments⁴ show the existence of a weak antiferromagnetic component in the direction of the c axis, which was predicted by Moriya⁵ in terms of the antisymmetric superexchange interaction. However, the magnitude of the canted component has not yet been determined.

Noting that the Cu hyperfine field⁶ associated with the Cu^{2+} ion in the octahedral crystal field depends on the direction of the Cu^{2+} spin with respect to the principal axis of tetragonal symmetry, we planned to clarify the canted structure by investigating the Cu NMR of the Cu^{2+} ions in $\text{CuCl}_2 \cdot 2\text{H}_2\text{O}$, whose spins couple antiferromagnetically.

The $\text{CuCl}_2 \cdot 2\text{H}_2\text{O}$ crystal belongs to an orthorhombic structure⁷ in space-group $Pbmn$ with two inequivalent Cu^{2+} ions at the positions $(0,0,0)$ and $(\frac{1}{2}, \frac{1}{2}, 0)$. The two oxygens coming from the two water molecules are coordinated axially to the Cu^{2+} ion completing, together with the 4Cl^- ions, an elongated octahedron with roughly tetragonal symmetry whose axes are denoted by (X, Y, Z) or (X', Y', Z') (Fig. 1). The tetragonal symmetry axis (Z or Z') is parallel to an axis of the Cl^- ions, which is inclined in the a - c plane by a 38° angle from the c axis.

The spin-echo method was employed for the Cu NMR measurements on $\text{CuCl}_2 \cdot 2\text{H}_2\text{O}$ single crystals at 1.5 K. After improvement of the weak spin-echo intensity by placing a larger number of single crystals into the resonance coil, two sets of quadrupole-split Cu NMR, central transition ($\pm \frac{1}{2} \leftrightarrow \mp \frac{1}{2}$), together with the satellites ($\pm \frac{1}{2} \leftrightarrow \pm \frac{3}{2}$), were observed in zero external field (Fig.

2). The two sets were assigned from numerical calculations to arise from two isotopic nuclei, ^{63}Cu and ^{65}Cu , respectively.

The dependence of the Cu NMR frequencies on the external field was also investigated using a small $\text{CuCl}_2 \cdot 2\text{H}_2\text{O}$ crystal ($2 \times 2 \times 30$ mm³) at 1.5 K, when an external field less than 8 kOe was applied along the a axis (Fig. 3). The twofold degeneracy of the Cu NMR frequency of Cu^{2+} ions associated with the antiferromagnetic sublattices was removed by applying an external field, i.e., with increasing external field one branch decreases while the oth-

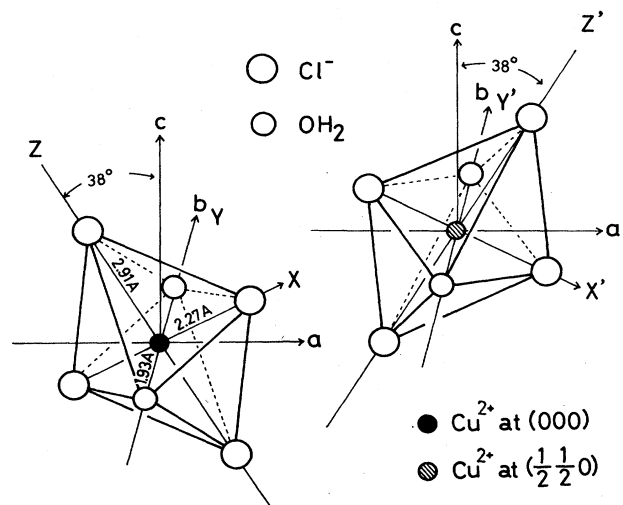


FIG. 1. Inequivalent Cu^{2+} ions at the $(0,0,0)$ and $(\frac{1}{2}, \frac{1}{2}, 0)$ positions in the orthorhombic unit cell of $\text{CuCl}_2 \cdot 2\text{H}_2\text{O}$, and their octahedral environments with roughly tetragonal symmetry. The principal axes of the crystal field for the central Cu^{2+} ion are represented by (X, Y, Z) or (X', Y', Z') . The local tetragonal axis, Z or Z' , inclines in the a - c plane by 38° from the c axis.

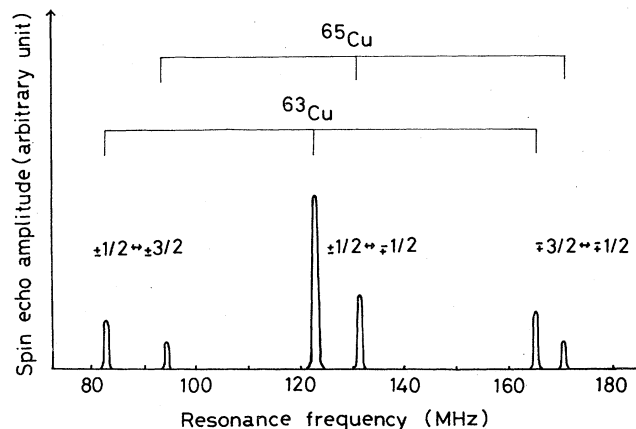


FIG. 2. Spin-echo spectra of Cu NMR ($I = \frac{3}{2}$) in single-crystal $\text{CuCl}_2 \cdot 2\text{H}_2\text{O}$ observed at 1.5 K in zero external field. The two sets of resonance absorptions correspond to the quadrupole-split transitions of the ^{63}Cu and the ^{65}Cu nuclei, respectively.

er branch increases.⁸ Though both branches were easily observed for external fields between 5 and 6.5 kOe, they were hard to detect at lower fields. The tendency was remarkable for the increasing branch. After a gradual change of the Cu NMR frequencies versus the external field H_0 up to about 6.5 kOe, all frequencies changed abruptly to low values at $H_0 = 6.6$ kOe. This corresponds to the change of the pre-

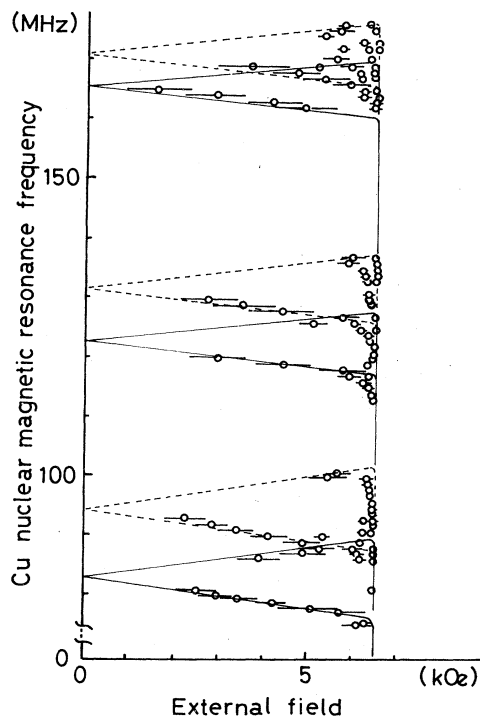


FIG. 3. External field dependence of the quadrupole-split ^{63}Cu and ^{65}Cu NMR frequencies (slashed circles) at 1.5 K in $\text{CuCl}_2 \cdot 2\text{H}_2\text{O}$, where the external field was applied along the a axis. The solid lines represent the NMR frequencies calculated for ^{63}Cu nuclei and the dotted ones those for ^{65}Cu nuclei using the zero-field values of (H_N, θ') and ν_Q in the text. The abrupt change of the Cu NMR frequencies at $H_0 = 6.6$ kOe corresponds to the spin-flop transition.

ferred spin axis from the a axis to the b axis at the critical field ($H_c = 6.6$ kOe), i.e., the spin-flop transition. When the Cu^{2+} spin \mathbf{S} lies parallel to the b axis (\mathbf{S} is perpendicular to the local tetragonal axis), the hyperfine field yields the minimum value, as will be discussed later. This is the reason why the Cu NMR frequencies drastically shift to low values at the spin-flop transition.

The Cu NMR frequencies in antiferromagnetic $\text{CuCl}_2 \cdot 2\text{H}_2\text{O}$, with or without the external field H_0 , can be evaluated from the calculation of the eigenvalue of the nuclear Hamiltonian \mathcal{H}_n via the following:⁶

$$\mathcal{H}_n = \mathcal{H}_z + \mathcal{H}_Q, \quad (1)$$

with

$$\mathcal{H}_z = \mathcal{H}_{\text{hyp}} + \mathcal{H}_0 = -\gamma\hbar\mathbf{I} \cdot \mathbf{H}_N - \gamma\hbar\mathbf{I} \cdot \mathbf{H}_0 = -\gamma\hbar\mathbf{I} \cdot \mathbf{H}$$

and

$$\mathcal{H}_Q = [eV_{zz}Q/[4I(2I-1)]]\{3I_z^2 - I(I+1) + \eta(I_x^2 - I_y^2)\},$$

where \mathcal{H}_z is the nuclear Zeeman interaction and \mathcal{H}_Q the nuclear quadrupole interaction. For the case where the total field $\mathbf{H} = \mathbf{H}_N + \mathbf{H}_0$ acting on the Cu nucleus always lies in the Z - X plane, one can reasonably simplify the quadrupole interaction to the case of $\eta = 0$ in \mathcal{H}_Q . Then, the eigenvalue equation for (1) can be solved numerically⁹ under a given choice of parameters ($\epsilon_z, \epsilon_Q, \theta''$), where $\epsilon_z = h\nu_z = \gamma\hbar H$, $\epsilon_Q = h\nu_Q = eV_{zz}Q/[2I(2I-1)]$, and $\theta'' = \arccos(\mathbf{H} \cdot \mathbf{Z}/H_Z)$. The analysis of the observed Cu NMR frequencies was carried out utilizing the numerical solution.

For the case of $H_0 = 0$ the best fit (Table I) between the observed three-quadrupole-split Cu NMR frequencies and the calculated ones was obtained using the values

$$H_N = -109.13 \pm 0.02 \text{ kOe},$$

$$\theta' = \arccos(\mathbf{H}_N \cdot \mathbf{Z}/H_N Z) = 10.3^\circ \pm 0.5^\circ,$$

$$\nu_Q = 14.49 \pm 0.05 \text{ (}^{63}\text{Cu)} \text{ and } 13.39 \pm 0.05 \text{ (}^{65}\text{Cu)} \text{ MHz}.$$

In the calculation we adopted $^{63}\nu_Q/^{65}\nu_Q = ^{63}Q/^{65}Q = 1.08$ (Ref. 10) and $^{63}\nu/^{65}\nu = ^{63}\gamma/^{65}\gamma = 0.934$ as the nuclear parameters for the two isotopic nuclei of copper.

On the other hand, introducing the parameters (A_{ZZ}, A_{XX}), parallel to the Z axis and to the X axis, respectively, as the principal values of the hyperfine tensor \hat{A} for the Cu^{2+} ion, the corresponding components (H_{ZZ}, H_{XX}) of the hyperfine field \mathbf{H}_N can be expressed with the relation $H_{ii} = A_{ii} \langle S \rangle$ in the same units. Then, when the Cu^{2+} spin

TABLE I. Observed and calculated values of the quadrupole-split Cu NMR frequencies for zero external field. The calculation was carried out in a straightforward fashion, as mentioned in the text, by using the values $H_N = -109.13$ kOe, $\theta' = \arccos(\mathbf{H}_N \cdot \mathbf{Z}/H_N Z) = 10.3^\circ$, and $\nu_Q = eV_{zz}Q/[2I(2I-1)h] = 14.49$ (^{63}Cu), 13.39 (^{65}Cu) MHz.

		Transitions (MHz)		
		$\pm \frac{3}{2} \leftrightarrow \pm \frac{1}{2}$	$\pm \frac{1}{2} \leftrightarrow \mp \frac{1}{2}$	$\mp \frac{1}{2} \leftrightarrow \mp \frac{3}{2}$
^{63}Cu	obs.	83.01 ± 0.20	122.60 ± 0.20	165.36 ± 0.20
	calc.	83.01	122.62	165.35
^{65}Cu	obs.	94.44 ± 0.20	131.39 ± 0.20	170.66 ± 0.20
	calc.	94.45	131.36	170.69

TABLE II. Dimensions of the octahedral environments of the Cu²⁺ ion and the principal values of the \bar{g} tensor in CuCl₂·2H₂O in comparison with those in K₂CuCl₄·2H₂O. The principal axes (X,Y,Z) are those shown in Fig. 1.

	CuCl ₂ ·2H ₂ O	K ₂ CuCl ₄ ·2H ₂ O
Octahedron (Å)		
OX (Cu-Cl)	2.27 ^a	2.22 ^b
OY (Cu-OH ₂)	1.93 ^a	1.85 ^b
OZ (Cu-Cl)	2.91 ^a	2.86 ^b
\bar{g} tensor		
g_{XX}	2.102 ^c	2.107 ^b
g_{YY}	2.047 ^c	2.047 ^b
g_{ZZ}	2.331 ^c	2.339 ^b

^aReference 7. ^bReference 12. ^cReference 13.

makes an angle θ with the tetragonal axis Z the magnitude and the direction, defined by an angle θ' , of the hyperfine field are given by^{6,11}

$$H_N(\theta) = (H_{ZZ}^2 \cos^2 \theta + H_{XX}^2 \sin^2 \theta)^{1/2}, \quad (2)$$

$$\tan \theta' = (H_{XX} / H_{ZZ}) \tan \theta.$$

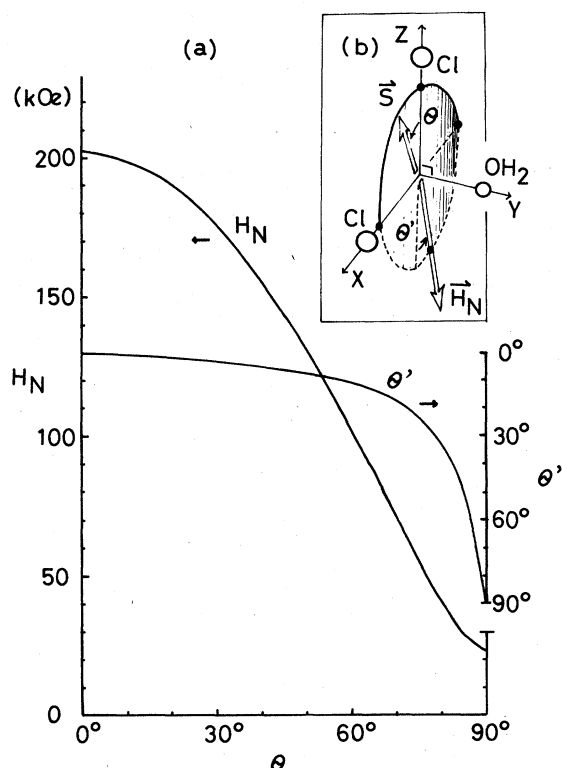


FIG. 4. (a) Angular dependence of the Cu hyperfine field and the angle $\theta' = \arccos(\mathbf{H}_N \cdot \mathbf{Z} / H_N Z)$ with respect to θ in the Z-X plane for the Cu²⁺ ion in CuCl₂·2H₂O, where θ is the angle between the direction of the Cu²⁺ spin \mathbf{S} and the Z axis. In terms of relation (2) in the text, the values (H_N, θ') were deduced from the principal values of the hyperfine tensor, $(A_{ZZ}, A_{XX}) = (-229.0, -25.2)$ in MHz, obtained by Looyestijn *et al.* (Ref. 12) for K₂CuCl₄·2H₂O in which the Cu²⁺ ions are quite similarly coordinated by 4Cl⁻ and 2H₂O in comparison with those in CuCl₂·2H₂O. (b) Cu²⁺ spin \mathbf{S} and the hyperfine field \mathbf{H}_N .

The two parameters (A_{ZZ}, A_{XX}) of the hyperfine tensor for the Cu²⁺ ion surrounded octahedrally by 4 Cl⁻ and 2 H₂O have been obtained for K₂CuCl₄·2H₂O by Looyestijn, Klaassen, and Poulis.¹² For both CuCl₂·2H₂O (Ref. 13) and K₂CuCl₄·2H₂O the same octahedral environments around the Cu²⁺ ion are realized, and the principal values of the \bar{g} tensor for the Cu²⁺ also have nearly the same magnitude, as shown in Table II. We can, therefore, adopt the same hyperfine field parameter for Cu nuclei in CuCl₂·2H₂O as for those in K₂CuCl₄·2H₂O, provided that the spin reduction and the supertransferred hyperfine field are neglected:¹²

$$(H_{ZZ}, H_{XX}) = (-202.6 \text{ kOe}, -22.3 \text{ kOe}). \quad (3)$$

Then, the hyperfine field $H_N(\theta)$ and the angle θ' expected for Cu²⁺ ions in CuCl₂·2H₂O can be calculated according to relation (2). These are shown with respect to the angle $\theta = \arccos(\mathbf{S} \cdot \mathbf{Z} / SZ)$ in Fig. 4. The observed values

$$(H_N, \theta') = (-109.13 \text{ kOe}, 10.3^\circ)$$

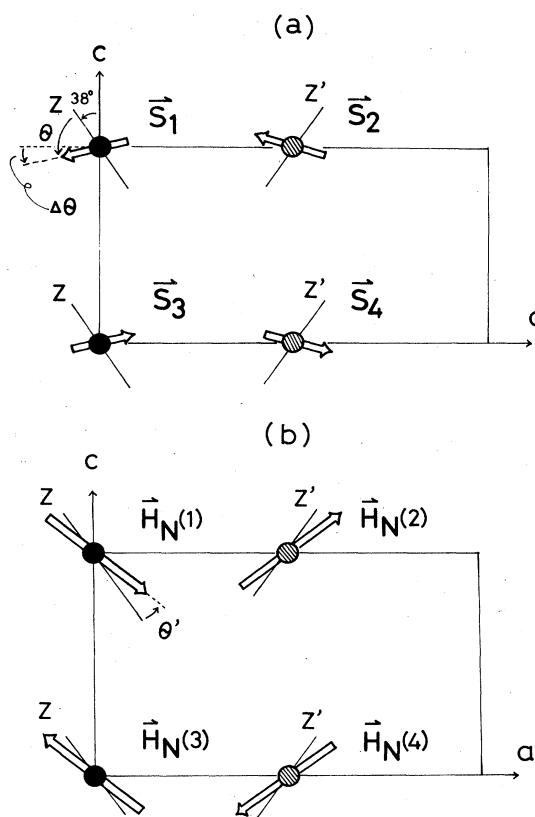


FIG. 5. (a) Antiferromagnetic structure of CuCl₂·2H₂O in the four-sublattice model where all spins are in the a-c plane. The canting angle $\Delta\theta$ was determined to be $6 \pm 1^\circ$ in the present investigations. There is a mutual correspondence between the local tetragonal axes (Z,Z') and the canting directions $\pm \Delta\theta$ away from the a axis. The black circles represent Cu²⁺ ions at the position (0,0,0) and the shaded circles ions at $(\frac{1}{2}, \frac{1}{2}, 0)$ in the orthorhombic unit cell. (b) Configuration of the hyperfine field $\mathbf{H}_N(i)$ corresponding to the Cu²⁺ spin \mathbf{S}_i . The angle θ' between \mathbf{H}_N and the tetragonal axis was determined to be 10.3° in the present Cu NMR measurements. \mathbf{H}_N and θ' are common in magnitude throughout the sublattices.

for the Cu nuclei in $\text{CuCl}_2 \cdot 2\text{H}_2\text{O}$ agree well with the case $\theta = 58^\circ$ in Fig. 4. Within the experimental accuracy, therefore, the canting angle $\Delta\theta$ in $\theta = 52^\circ + \Delta\theta$ can be deduced to be $6^\circ \pm 1^\circ$. The present result can be understood as follows: the antiferromagnetic sublattices in $\text{CuCl}_2 \cdot 2\text{H}_2\text{O}$ cant each other by 6° in the a - c plane away from the a axis, taking into account the qualitative result of spin canting in the a - c plane determined through neutron diffraction measurements.⁴ The four-sublattice structure deduced is illustrated in Fig. 5(a), together with the local tetragonal axes Z and Z' . In this configuration, though \mathbf{S} makes one of four kinds of directions with respect to the a axis in the crystal, the angle θ between Z and \mathbf{S} is common in magnitude, since there is a mutual correspondence between the directions of \mathbf{S} and the local tetragonal axes. The existence of the common θ for all spins in $\text{CuCl}_2 \cdot 2\text{H}_2\text{O}$ crystal at $H_0 = 0$ implies a unique value of (H_N, θ') for the Cu nuclei, as has indeed been observed. The resulting configuration of the hyperfine field vector \mathbf{H}_N in $\text{CuCl}_2 \cdot 2\text{H}_2\text{O}$ is illustrated in Fig. 5(b).

For the case of the applied field along the a axis the values of the Cu NMR frequencies calculated using both the zero-field values of (H_N, θ') and those of ν_Q are depicted in Fig. 3 as solid lines for ^{63}Cu and dotted ones for ^{65}Cu , which agree well with the observed points. With the application of \mathbf{H}_0 along the a axis, the total fields $\mathbf{H} = \mathbf{H}_N + \mathbf{H}_0$ acting on the Cu nuclei associated with the \mathbf{S}_1 sublattice and those associated with the \mathbf{S}_2 sublattice in Fig. 5 are both not only symmetric with respect to the a axis but also equal in magnitude. Similar relations hold for the total fields acting

on Cu nuclei associated with the \mathbf{S}_3 and the \mathbf{S}_4 sublattices in Fig. 5. With increasing H_0 , therefore, the frequency of the Cu nucleus subjected to the former effective field is expected to increase while that subjected to the latter is expected to decrease, or vice versa. This is the reason why, in presence of H_0 along the a axis of magnitude less than 6.6 kOe, the Cu NMR frequency splits into two branches, as shown in Fig. 3.

Since the highest symmetry element between the Cu^{2+} ions at $(0,0,0)$ and those at $(\frac{1}{2}, \frac{1}{2}, 0)$ is a twofold rotation axis perpendicular to the line joining the ions, the vector \mathbf{D} , representing the antisymmetric superexchange interaction $\mathbf{D} \cdot (\mathbf{S}_1 \times \mathbf{S}_2)$, is restricted to the a - b plane, i.e., $\mathbf{D} = (D_a, D_b, 0)$, where the effect of D_a can be considered negligible¹⁴ because the spin cant caused by D_a is an order of magnitude smaller than that caused by D_b . In this case, the magnitude of D_b can be evaluated from the relation $\tan(2\Delta\theta) = |D_b|/2J'$ as 0.28 K, adopting the ferromagnetic superexchange interaction $J' = 0.67$ K (Ref. 15) between the next nearest-neighbor Cu^{2+} ions in the a - b plane. The canted component of the Cu^{2+} spin amounts to nearly 10% of the a component, which is consistent with Moriya's estimation.⁵

The authors would like to express their sincere thanks to Professor H. Yasuoka, Professor K. Motizuki, and Dr. T. Goto for valuable discussions. Thanks are also due to Professor A. Hirai for continual encouragement.

¹N. J. Poulis and G. E. G. Hardeman, *Physica* **18**, 315 (1952).

²C. J. Gorter and J. Haantjes, *Physica* **18**, 285 (1952).

³J. Ubbink, J. A. Poulis, H. J. Gerritsen, and C. J. Gorter, *Physica* **18**, 361 (1952); **19**, 928 (1953).

⁴H. Umebayashi, B. C. Frazer, D. E. Cox, and G. Shirane, *Phys. Rev.* **167**, 519 (1968).

⁵T. Moriya, *Phys. Rev.* **120**, 91 (1960).

⁶A. Abragam and B. Bleaney, *Electron Paramagnetic Resonance of Transition Ions* (Clarendon, Oxford, 1970), Chaps. 3 and 7; M. Fujii, F. Wakai, H. Abe, and A. Hirai, *J. Phys. Soc. Jpn.* **50**, 1109 (1981).

⁷S. W. Peterson and H. A. Levy, *J. Chem. Phys.* **26**, 220 (1957).

⁸T. Kubo, K. Adachi, M. Mekata, and A. Hirai, *Solid State Com-*

mun. **29**, 553 (1979).

⁹P. M. Parker, *J. Chem. Phys.* **24**, 1906 (1956).

¹⁰H. Krüger and U. Meter-Berkhout, *Z. Phys.* **132**, 171 (1952).

¹¹L. D. Khoi and P. Veillet, *Phys. Rev. B* **11**, 4128 (1975).

¹²W. J. Looyestijn, T. O. Klaassen, and N. J. Poulis, *Physica* **66**, 567 (1973); T. O. Klaassen, W. J. Looyestijn, and N. J. Poulis, *ibid.* **101B+C**, 53 (1980).

¹³E. Buluggiu, G. Dascola, D. C. Giori, and A. Vera, *J. Chem. Phys.* **54**, 2191 (1971).

¹⁴R. J. Joenk, *Phys. Rev.* **126**, 565 (1962).

¹⁵M. Date, M. Motokawa, A. Seki, S. Kuroda, K. Matsui, H. Nakazato, and H. Molymoto, *J. Phys. Soc. Jpn.* **39**, 565 (1975).